J Fluoresc (2014) 24:639–648
DOI 10.1007/s10895-013-1337-0

ORIGINAL PAPER

NO Fluorescence Quantification by Chitosan CdSe Quantum Dots Nanocomposites

Eliana F. C. Simões · João M. M. Leitão · Joaquim C. G. Esteves da Silva

Received: 14 October 2013 / Accepted: 20 November 2013 / Published online: 11 December 2013

Abstract The quantification of nitric oxide (NO) based on the quenching of the fluorescence of a nanocomposites sensor constituted by cadmium/selenium quantum dots (CdSe) stabilized by chitosan (CS) and mercaptosuccinic acid (MSA) is assessed. The optimization of the response of the CS-CdSe-MSA nanocomposites to NO was done by multivariate response surface experimental design methodologies. The highest fluorescence quenching was obtained at pH 5.5 and at room temperature. The NO quantification capability of CS-CdSe-MSA was evaluated using standard solutions and a NO donor reagent. A large linear working range from 5 to 200 μM and a limit of detection of 1.86 μM were obtained. Better quantification results were obtained using the NO donor reagent. Besides NO, the response of the fluorescence of CS-CdSe-MSA to the main reactive oxygen and nitrogen species and similar NO compounds was also assessed.

Keywords Nitric oxide · Chitosan · Quantum dots · Nanocomposites · Fluorescence · Quenching

Introduction

Reactive oxygen species (ROS), as superoxide ($O_2^{\cdot-}$) and hydrogen peroxide (H_2O_2), and reactive nitrogen species (RNS), as nitric oxide (NO) and peroxynitrite ($ONOO^-$), are usually involved in several physiological and pathological processes acting as a signalling molecule. However at higher concentrations these reactive species induce cell damage. Their determination is a matter of great importance in the study of various physiological and pathological processes [1]. Due to their high reactivity, short half-life, lower concentrations, rapid diffusion, possible antioxidant mechanisms and potential interferences, their quantification and/or detection is a continuous challenge. Also the chemistry of these species, namely the preparation and manipulation of standard and sample solutions, is not straightforward due to their reactivity and trace amounts in biological fluids [2,3].

Nitric oxide (NO) and other ROS/RNS regulate many biological processes, such as cardiovascular relaxation, nervous transmission and immunological responses. Disturbs in the NO pathway can provoke disorders such as central nervous system disorders, diabetes mellitus, stroke, hypertension, cardiac failures and others. Due to this regulator role, NO is one of the most studied ROS/RNS and is object of an intense research in order to adequately detect and/or quantify NO by different analytical techniques. The main analytical techniques used are electron spin resonance, chemiluminescence, fluorimetric, colorimetric and electrochemical [2–5]. The fluorescence detection and/or quantification of NO have been done essentially by several classes of organic fluorophores as diaminofluoresceins, diaminorhodamines, dihydrorhodamines, diaminonaphthalene and diaminoanthraquinones [2–7].

Some sensors based in nanocrystalline semiconductors quantum dots (QDs) have been developed as fluorescent probes for NO [8–14]. Most of these sensors are based in CdSe [8–13] and one is based in the CdTe [14] QDs. Also most of the CdSe sensors are based in the quenching of fluorescence [8–12] and only one is based in the enhancement of fluorescence [13]. Sensors based in CdSe fluorescence quenching for NO detection were coupled to fiber optics using cellulose acetate sensitive membranes [8]; biocompatible

E. F. C. Simões · J. M. M. Leitão
Faculdade de Farmácia da Universidade de Coimbra, Pólo das Ciências da Saúde, Centro de Investigação em Química da Universidade do Porto (CIQ-UP), 3000-548, Coimbra, Portugal

J. C. G. Esteves da Silva (✉)
Departamento de Química, Faculdade de Ciências da Universidade do Porto, Centro de Investigação em Química da Universidade do Porto (CIQ-UP), R. Campo Alegre 687, 4169-007 Porto, Portugal
e-mail: jcsilva@fc.up.pt

CdSe QDs chitosan (CS) nanocomposites [9]; CdSe/ZnS QDs in polymethacrylate films [10]; CdSe QDs prepared by changing the oleic acid with tiethanolamine [11]; CdSe QDs coating with metalloporfirins films [12]. Sensor based in the fluorescence enhancement are based in CdSe/ZnS QDs functionalized with tris(dithiocarbamato)iron(III) [13]. A sensor based in CdTe QDs was developed by linked to carboxymethyl chitosan (CMCS) [14]. For the two NO sensors based in CS nanocomposites a linear working range from 5 to 55 μM for CS-CdSe [9] and from 4.6 to 55.2 μM for CMCS-CdTe [14] were obtained.

Nanocomposites resulting of the combination of inorganic molecules with organic molecules (biopolymers as CS) have been used in diagnosis and in cell targeted drug delivery. Indeed chitosan is a biocompatible and biodegradable biopolymer with reduced cytotoxicity and low immunogenicity with a great potential to be used in biomedical applications [15,16]. The combination of QDs and CS allows increasing their biocompatibility and consequently their use in bioapplications. Other nanocomposites composed by QDs and CS, or its derivatives, have been reported [16–18].

In this work, a new CS-CdSe-MSA nanocomposites was synthesized and the potential as NO quantitative sensor was optimized and evaluated. Optimization using response surface experimental design methodologies were used in order to establish the more adequate conditions to the NO quantification by CS-CdSe-MSA. The more adequate pH and temperature conditions for the NO fluorescence sensing with the CS-CdSe-MSA were obtained. In the optimized conditions, the NO detection capability was checked varying the NO concentration and the quantification capability was evaluated in standard solutions and by the generation of NO with a rapid donor diethylamine NONOate (DEA/NO).

Experimental

Reagents

Analytical grade reagents were used: mercaptossucinic acid (MSA), acetic acid, sodium hydroxide (NaOH), sodium borohydride ($NaBH_4$), sodium nitrite, hydrogen peroxide (H_2O_2), hydrogen chloride (HCl), potassium superoxide (KO_2), diethylamine/nitric oxide complex sodium (DEA/NO), sodium nitrate ($NaNO_3$) and sodium nitrite ($NaNO_2$). A low-molecular weight chitosan (CS) sample with a degree of deacetylation greater or equal to 75 % was used (Sigma-Aldrich). Mili-Q water with a resistivity 18 MΩ.cm at 25 °C was used.

Solutions

A CS solution working solution was obtained by filtration of an aqueous solution resulting from the dissolution of 5 g of CS in 500 mL of 0.1 M acetic acid. A hydrogen selenide solution was prepared by mixing 58 mg of Se and 73 mg of $NaBH_4$ with 3 mL of deoxygenated water and kept under nitrogen.

CdSe QDs capped with MSA were prepared by the following procedure: 171 mg of MSA was dissolved in H_2O (50 mL) and the pH was adjusted to 7.0 using a NaOH aqueous solution; next, 28 mg of $CdCl_2$ was added and the pH was again adjusted to 7.0; finally, 200 μL of a hydrogen selenide solution was added to this solution, with continuously stirring yielding an yellow-orange solution.

CS-CdSe-MSA nanocomposites were obtained by the following procedure: 684 mg of MSA was dissolved in H_2O (200 mL) and the pH was adjusted to 7.0 using a NaOH aqueous solution; 112 mg of $CdCl_2$ was added to the previously MSA solution and the pH was again adjusted to 7.0; next, 200 mL of the CS solution was added to the previous solution and well mixed; finally, 1 mL of a hydrogen selenide solution was added to that mixture under a strong continuously stirring, yielding an yellow solution. This mixture was kept under strong stirring for 24 h and it was dialysed for several days against deionised water using a cellulose membrane dialysis tubing (reference D9652 from Sigma). The purified nanocomposites solution is the sensor solution and was stable at room temperature.

Saturated NO solutions (1.9 mM) were prepared by bubbling NO in deoxygenated water, after bubbling argon for 15 min. Standard solutions were prepared in deoxygenated water by rigorous dilution. The DEA/NO stock solution was prepared in NaOH 10 mM and kept at 20 °C before use.

The solutions of H_2O_2, KO_2, $NaNO_3$, $NaNO_2$ were prepared in water. Deoxygenated water was used for the preparation of H_2O_2 and KO_2 solutions. Also solutions of HCl and NaOH 0.1 M were prepared in order to evaluate the influence of pH in the response of the nanocomposites to NO.

Instrumentation

Evaluations were made using a QE65000 charge-coupled detector, a 380 nm light emitting diode (LED), a sampling compartment (CUV-ALL-UV 4-way) and two 1.0 mm core diameter fiber optics (P1000-2-UV–VIS) from Ocean Optics. One of the fibers guides the light from the source to the sampling compartment and the other guide the emitted light to the detector. The reaction time profiles were obtained collecting the signal at the maximum emission wavelength, every 10 s with an integration time of 300 ms. A difference between the initial and the final fluorescence intensity measured after 10 min the addition of NO (intensity variation) were used in all the work.

The absorbance and fluorescence spectra were obtained in a standard 1 cm fluorescence quartz cell and collected respectively in a Jasco V-530 UV-Visible spectrophotometer and in a Jasco FP-6200 spectrofluorimeter. The absorption spectra

were obtained in a wavelength range from 250 to 650 nm with a 2 nm interval, slit widths 2 nm and wavelength scan rate medium; the Fluorescence spectra were obtained in a wavelength range from 300 to 700 nm with a 1 nm interval, slit widths 5 nm, sensitivity response medium, response time fast and wavelength scan rate 1000 nm/min.

The particle size of QDs and nanocomposites and their distribution was obtained by DLS in a Nano Delsa C, Beckman Coulter and by transmission electronic microscopy (TEM) in a FEI Company Tecnai G2 20 S-Twin electronic microscopic. The shape of the particles was also determined by TEM analysis.

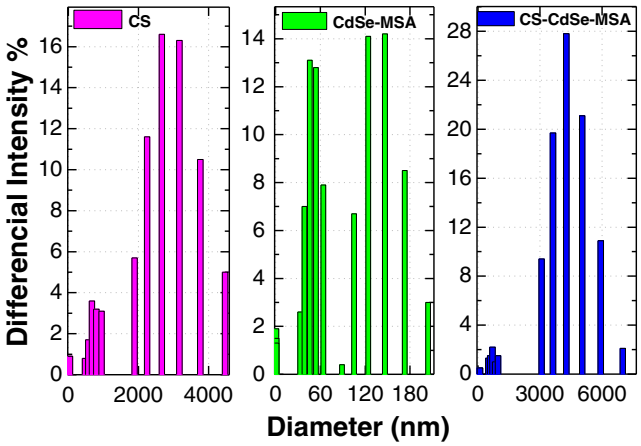

Fig. 2 Particle size distribution of CS, CdSe-MSA and CS-CdSe-MSA obtained by DLS

Data Analysis

The quantum yield (Φ) of the CdSe-MSA QDs and CS-CdSe-MSA nanocomposites were calculated comparing the integrated photoluminescence intensities and the absorbance values of the nanocomposites with the ones of the quinine sulfate [21].

$$\Phi = \Phi_R \times \frac{Grad}{Grad_R} \times \frac{\eta^2}{\eta_R^2}$$

In the equation Φ is the fluorescence quantum yield, Grad is the gradient from the plot of integrated fluorescence intensity *vs*. absorbance and η is the refractive index. The subscripts R refer to reference fluorophore, quinine sulfate of known quantum yield. The Φ of the quinine sulfate is Φ= 0.54. The η of the quinine sulfate in 0.1 M H_2SO_4 and of nanocomposites water solutions used were η=1.33.

A central composite experimental design (CCD) was used for the response surface optimization. This experimental design allows the identification of the optimum response. It also allows the assessment of the significance of the effects of design variables and interactions without confusing their effects. In order to obtain an estimate of errors, a center experiment is included in the experimental design in which the average value

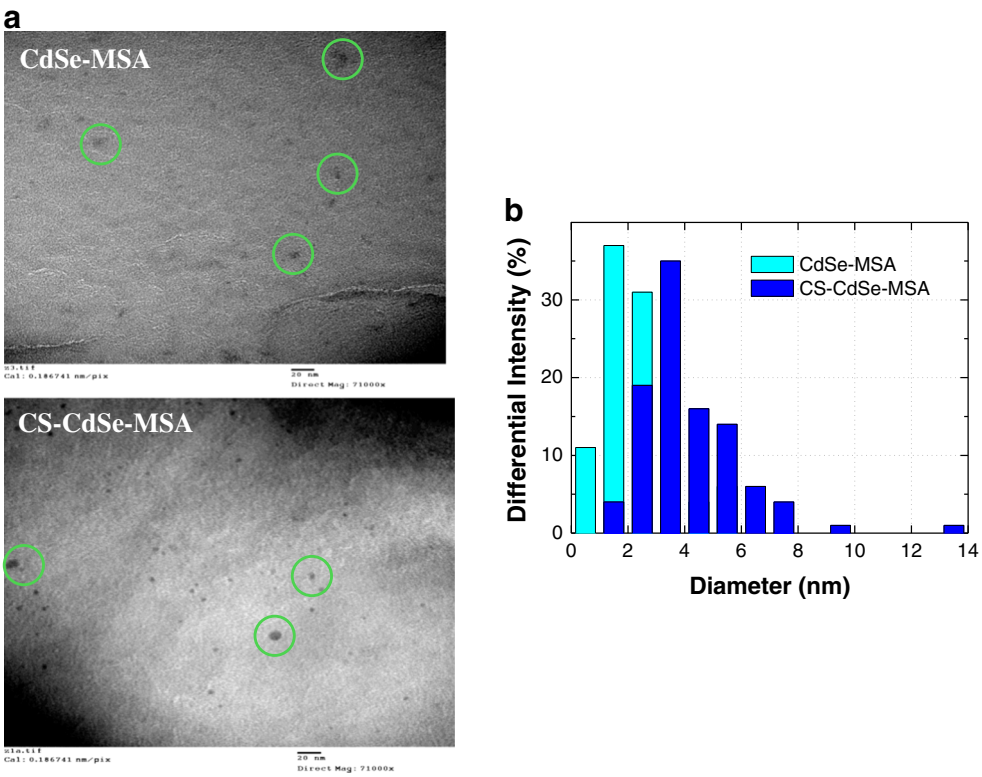

Fig. 1 TEM images (**a**) and particle size distribution plots (**b**) of CdSe-MSA and CS-CdSe-MSA nanocomposites

Table 1 Frequency table of particle size distribution of CS, CdSe-MSA and CS-CdSe-MSA obtained by DLS

Particle size			
	D 10 %	D 50 %	D 90 %
CS	707	2686	44792
CdSe-MSA	35	92	167
CS-CdSe-MSA	2658	3890	5275

of all variables is used. The assessment of the significance of the effects of the design variables and interactions, global linear model, global model quadratic effects and response surfaces was made by analysis of variance (ANOVA) through F-ratio and respective p value. The value of multiple linear regression coefficients of design variables and interactions were also evaluated [19,20]. The CCD was implemented with the Unscrambler® software version 7.51, Camo ASA, Norway.

Results

Characterisation

The size distribution of the nanocomposites was characterized by TEM and DLS and, for comparison purposed, its two main constituents, CS and QDs, were also analyzed.

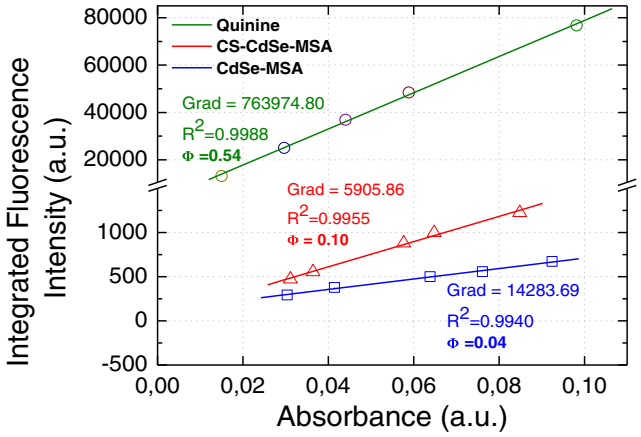

Fig. 4 Quantum yields determinations of CS-CdSe-MSA and CdSe-MSA

TEM

Figure 1 presents the micrographs and the particle core size distribution obtained by TEM analysis. An average particle core size of 2.24 nm (standard deviation - 1.20 nm) for the CdSe-MSA and of 4.19 nm (standard deviation - 1.83 nm) for the CS-CdSe-MSA was observed. This analysis shows that the core of the nanoparticles increases about two times when CS is present.

DLS

Figure 2 and Table 1 present the results, i.e. the size of particles considering the outer salvation sphere, obtained by

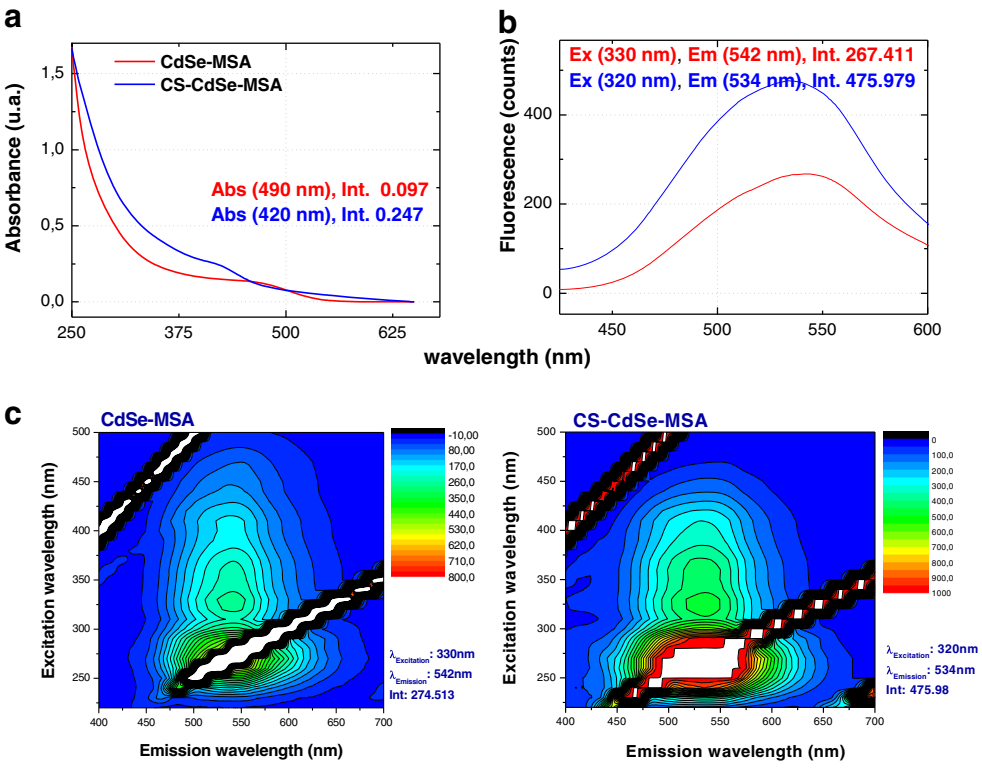

Fig. 3 Absorption (**a**), emission spectra (**b**) and EEM (**c**) of CdSe-MSA and CS-CdSe-MSA

Table 2 Levels of central composite experimental designs

Design variables	Cube levels		Central level
	Low	High	
Central composite design (pH 4-8)			
pH	5	8	6.500
Star levels – Low – 4.385; High –8.615			
Temperature (°C)	25	50	37.500
Star levels – Low – 19.875; High – 55.125			
Central composite design (pH 4-7)			
pH	4.5	6.5	5.500
Star levels – Low – 4.090; High – 6.910			
Temperature (°C)	25	50	37.500
Star levels – Low – 19.875; High – 55.125			

DLS for CS, CdSe-MSA and CS-CdSe-MSA nanoparticles. Taking into consideration the information provided by DLS, and that CS in water is extensively solvated, relatively high dimension particles are expected to be detected.

The analysis of size distribution of the hydrated nanoparticles presented in Fig. 2 shows that the raw QDs (CdSe-MSA) are characterized by nanosized hydrated particles, while when CS is presented (raw CS and the CS nanocomposites), the outer salvation spheres of the particles increase towards the micro-sized dimensions. These results confirm that CS in water is extensively hydrated (it is a gel) as well as the nanocomposites where it is presented.

UV and Fluorescence

Figure 3 shows the absorption and emission spectra and excitation emission matrices (EEM) of CdSe-MSA QDs and CS-CdSe-MSA nanocomposites. The analysis of the EEM shows that the presence of CS on the QDs surface has no significantly effect on photoluminescent properties of the QDs. Indeed, similar fluorescence excitation and emission wavelengths at maximum fluorescence intensity are observed for the QDs ($\lambda_{ExCitation}$ 320 nm, $\lambda_{Emission}$ 542 nm) and nanocomposites QDs (CdSe-MSA - $\lambda_{Excitation}$ 320 nm, $\lambda_{Emission}$ 542 nm; CS-CdSe-MSA - $\lambda_{Excitation}$ 320 nm, $\lambda_{Emission}$ 534 nm). Only a slightly UV-shift of the excitation wavelength and an increase of the fluorescence intensity with the incorporation of CS is observed. This is confirmed by the analysis of the absorption spectra of the two nanocomposites, where a hypsochromic shift, from 490 nm to 420 nm, and a more than two times increase of the absorbance is observed in the CS-CdSe-MSA nanocomposite.

Table 3 ANOVA results for the Δ fluorescent intensity response variable using a central composite optimization experimental design (pH 4 - 8)

ANOVA ($R_{Multiple}$=0.941)						
Effect	SS	d.f.	MS	F-ratio (*p*-value)	B	$(S.D.)_b$
Model	9.241×10^4	5	1.848×10^4	7.760 (0.021)		
Error	1.191×10^4	5	2.382×10^3			
Adjusted total	1.043×10^5	10	1.043×10^4			
Factor						
Intercept	5.120×10^4	1	5.120×10^4	21.497 (0.006)	-130.640	28.177
pH	6.505×10^4	1	6.505×10^4	27.312 (0.003)	60.206	11.520
Temperature	2.569×10^3	1	2.569×10^3	1.079 (0.347)	1.436	1.382
pH × Temp	789.889	1	789.889	0.332 (0.590)	11.209	19.463
pH × pH	2.400×10^4	1	2.400×10^4	10.076 (0.025)	52.208	16.447
Temp. × Temp.	1.900×10^3	1	1.900×10^3	0.789 (0.413)	14.688	16.447
Model check						
Main	6.762×10^4	2	3.381×10^4			
Int.	789.887	1	789.887	0.332 (0.590)		
Int. + Squ.	2.400×10^4	2	1.200×10^4	5.039 (0.063)		
Squ	2.400×10^4	2	1.200×10^4	5.039 (0.063)		
Error	1.191×10^4	5	2.382×10^3			
Lack of fit						
Lack of fit	1.009×10^4	3	3.362×10^3	3.688 (0.221)		
Pure error	1.823×10^3	2	911.692			
Total error	1.191×10^4	5	2.382×10^3			

RMultiple multiple correlation, *SS* sum of squares; *d.f.* degrees of freedom; *MS* mean squares; *F-ratio* Fisher ratio; *b* beta-regression coefficient; $(S.D.)_b$ standard deviation of b; *Main* main effects; *Int.* interactions effects; *Squ.* squares effects; *p-value* probability value (p) for a 5 % significance level

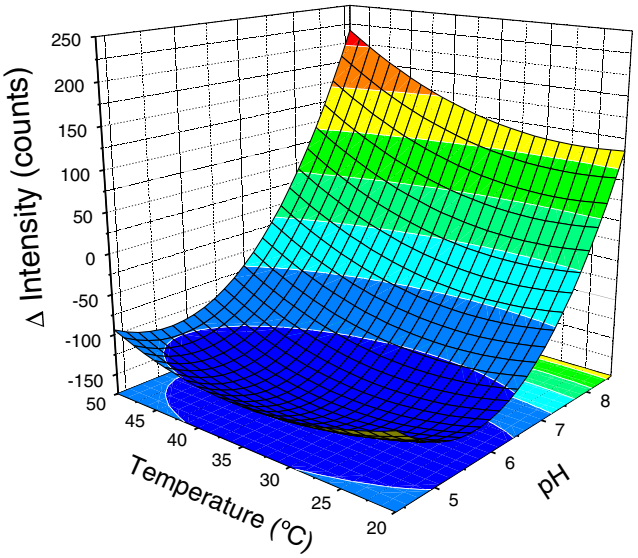

Fig. 5 Response surface fluorescence intensity obtained with the central composite experimental design for pH values between 4 and 8

Figure 4 shows the determination of the quantum yield of the nanoparticles. A relatively lower quantum yield was found for the two nanocomposites. Nevertheless the introduction of CS resulted in a more than two times increase of the Φ found for the CS-CdSe-MSA (Φ = 0.10) relatively of the Φ found for the CdSe-MSA (Φ = 0.04).

Optimization

The optimization of the response of CS-CdSe-MSA to NO was done by response surface methodology using central composite experimental designs (CCD). The evaluated experimental variables were the pH and temperature and the response variable was the difference between the initial and the final fluorescence intensity collected 10 s after the NO addition (Δ Intensity). Two CCD were done with a different pH range and similar temperature range (Table 2).

Table 3 shows the results obtained for the ANOVA of the fluorescence intensity variation as response variable and varying the pH from 4 to 8. Of the global analysis of the model it is possible to conclude that the model adequately fit the data. A statistically significant model (p =0.021), a non-statistically significant lack of fit (p =0.221) with a high $R_{Multiple}$=0.941 it's obtained. By analysis of this table the more relevant is the effect of the pH in the response variable. Indeed, the pH causes a statistically significant increase (p =0.003) of the fluorescence intensity variation and, due to the statistically significant pH square effect (p =0.025), a curvature of the response surface will be expected. Due to the precipitation of CS (pKa=6.5), and possible consequent destruction of the CS-CdSe-MSA structure at a pH higher than 7, a different response to NO with an increase of fluorescence is observed.

Table 4 ANOVA results for the Δ fluorescent intensity response variable using a central composite optimization experimental design (pH 4 - 7)

ANOVA ($R_{Multiple}$=0.978)						
Effect	SS	d.f.	MS	F-ratio (p-value)	B	$(S.D.)_b$
Model	1.094×10^3	5	218.725	21.993 (0.002)		
Error	49.726	5	9.945			
Ajusted total	1.143×10^3	10	114.335			
Factor						
Intercept	702.902	1	702.902	70.677 (0.0004)	-15.307	1.821
pH	635.214	1	635.214	63.871 (0.001)	8.924	1.117
Temperature	275.491	1	275.491	27.701 (0.003)	0.470	8.933×10^{-2}
pH × Temp	157.126	1	157.126	15.799 (0.011)	4.999	1.258
pH × pH	23.46	1	23.46	2.359 (0.185)	-1.632	1.063
Temp × Temp	8.256	1	8.256	0.830 (0.404)	-0.968	1.063
Model check						
Main	910.705	2	455.352			
Int.	157.126	1	157.126	15.799 (0.011)		
Int. + Squ.	25.796	2	12.898	1.297 (0.352)		
Squ	25.796	2	12.898	1.297 (0.352)		
Error	49.726	5	9.945			
Lack of fit						
Lack of fit	11.609	3	3.870	0.203 (0.887)		
Pure error	38.117	2	19.058			
Total error	49.726	5	9.945			

RMultiple multiple correlation, *SS* sum of squares; *d.f.* degrees of freedom; *MS* mean squares; *F-ratio* Fisher ratio; *b* beta-regression coefficient; $(S.D.)_b$ standard deviation of b; *Main* main effects; *Int.* interactions effects; *Squ.* squares effects; *p-value* probability value (p) for a 5 % significance level

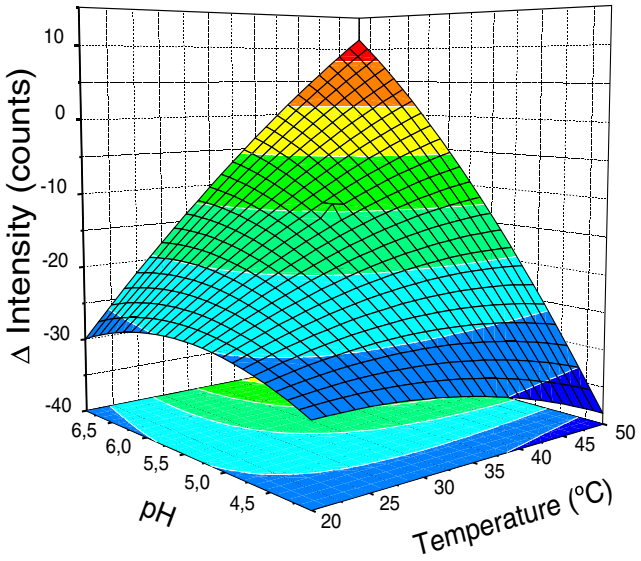

Fig. 6 Response surface fluorescence intensity obtained with the central composite experimental design for pH values between 4 and 7

Figure 5 shows the response surface obtained for the fluorescence intensity variation with the central composite design varying the pH from 4 to 8. The analysis of Fig. 5 confirms that the variable pH affects most significantly the response variable and that the temperature shows a lowest variability in the response variable in the studied range. This figure shows a region where the response variable presents minimum values corresponding to a maximum of fluorescence quenching. This minimum region is observed at a pH from 4.40 to 6.85 at all temperature range. A minimum value of the response variable intensity variation equal to -162.8 was predicted at pH 5.5 and temperature 34.6 °C.

Attending to these results a new central composite design was yet performed now in a pH range from 4 to 7 in the same range of temperatures (Table 2). Table 4 shows the results obtained for the ANOVA for the fluorescence intensity variation as response variable and varying the pH from 4 to 7. Of the global analysis of the model it is possible to conclude that the model adequately fit the data. A statistically significant model (p =0.002), a non-statistically significant lack of fit (p = 0.887) with a high $R_{Multiple}$=0.978 is obtained. By the analysis of this table it is possible to evaluate the statistically significant effects of the pH (p =0.001) and of temperature (p =0.003) in the response variable. Also the interaction between the two variables is statistically significant (p =0.011). Both experimental variables and the interaction induce an increase of the fluorescence intensity variation.

The Fig. 6 shows the response surface obtained for the variable Δ fluorescence intensity with the central composite design restricting the range of the variable pH between 4 and 7. By the analysis of Fig. 6 it is possible to see that there isn't a clearly region of a maximum or minimum of the response variable and even a predicted saddle point was evaluated. Nevertheless, it is possible to define a region of minimum avalues at a pH below 5 at all the temperature range and a region of maximum values at pH above 6.5 at temparature higher than 55 °C of the response variable.

Taking into consideration the relatively small interaction among the two variables a univariate optimization of the pH and temperature was done with a [NO]=50 μM in order to obtain more information about the optimal working regions. The pH was evaluated in a range from 5.5 to 8.5 at temperature 25 °C (Fig. 7) and the temperature was evaluated in a range from 20 to 50 °C at pH 5.5 (Fig. 8).

In Fig. 7, and as previous evaluated, an increase of Δ fluorescence intensity is observed at a basic pH. At pH 7.5 the fluorescence intensity remains almost constant, at pH 7 a lower variation it's observed and only at a pH below 6.5 it's observed the maximum fluorescence quenching. These results show that a stable region of maximum fluorescence quenching is situated at pH values between 5.5 and 6.5.

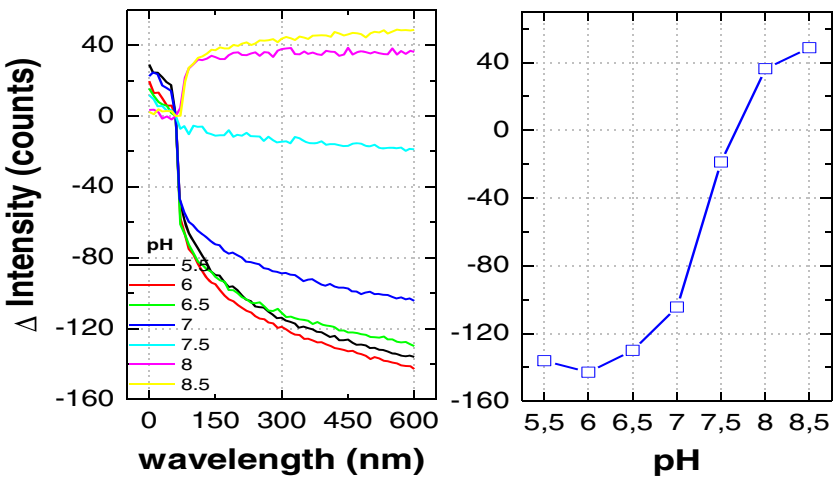

Fig. 7 Fluorescence intensity variation for pH variation at temperature 25 °C and [NO]=50 μM

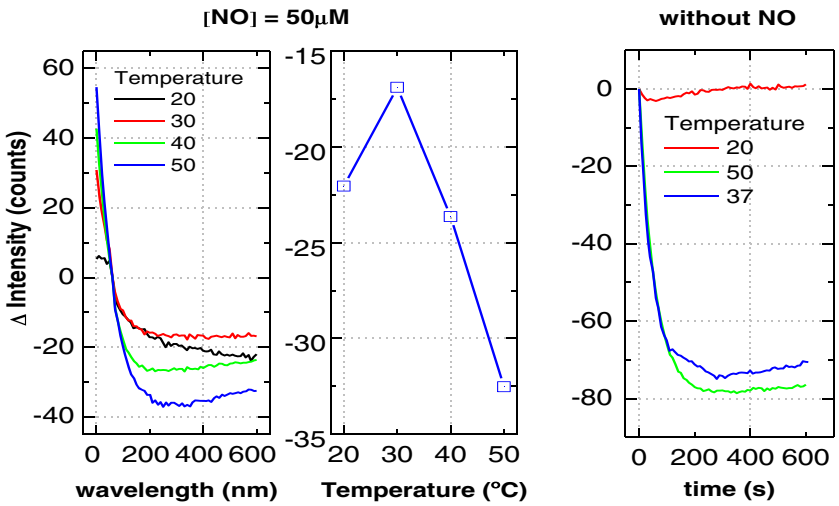

Fig. 8 Fluorescence intensity variation of CS-CdSe-MSA nanocomposite at different temperatures at pH 4.5 by addition of [NO]=50 μM and without NO

In Fig. 8 a small effect on the fluorescence intensity variation is observed in the temperature range evaluated. Nevertheless, the fluorescence intensity becomes somewhat smaller even without NO addition, which provoke a marked effect in the stability of the initial fluorescence intensity of the CS-CdSe-MSA nanocomposite. Consequently, a lower temperature is the more adequate for the NO fluorescence quenching. pH 5.5 and room temperature is the best reaction conditions in order to the NO quantification by the CS-CdSe-MSA.

Quantification of NO

Figure 9 shows typical reaction time profiles of fluorescence intensity variations of the CS-CdSe-MSA nanocomposite with addition of different NO concentrations under the optimized conditions (pH 5.5 and room temperature). From the analysis of Fig. 9 it is possible to observe a marked fluorescence quenching with the addition of NO. A very small variation of the fluorescence intensity of the CdSe-MSA QDs is observed with the addition of NO (data don't shown).

A linear decrease in the fluorescence intensity is observed in the presence of NO concentration from 1.00 to 200 μM. At a reaction time higher than 500 s a fluorescence intensity stabilization is observed. As shown in Table 5, a linear work range from 1 to 200 μM [y=-0.951x+3.856 (m=6); R= 0.99415] with a detection limit of 1.86 μM were obtained. Good quantification results were observed with the solutions under investigation. For the standard solutions and for the DEA/NO solution a recovery around 85 % and for DEA/NO solution of 92 % were found.

The comparison of the response of some ROS/RNS and other NO similar compounds were done in order to evaluate

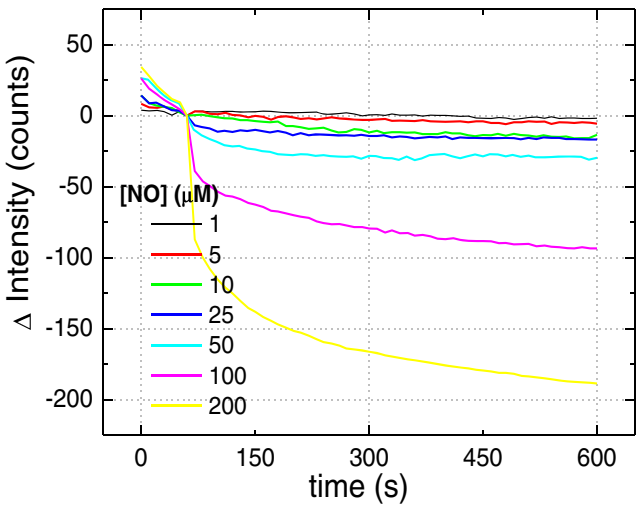

Fig. 9 Fluorescence time profiles of the reaction of CS-CdSe-MSA nanocomposite with NO at different concentrations

Table 5 NO quantification results in a NO donor solution and in standard solutions found by CS-CdSe-MSA in the optimized reaction conditions

NO quantification			
y=- 0.93x - 4.60; m=6; R^2=0.9961; s_a=2.75; s_b=0.03; $s_{y/x}$=4.87; [NO]=5 - 200 μM			
s_{blank}=2.05; LD_{sblank}=1.86 μM; LQ=6.00 μM			
	[NO]=25 μM	[NO]=50 μM	[DEA/NO]=25 μM
[NO] (μM)	20.30±16.10	42.21±15.80	34.45±15.90
Recovery (%)	83.99	84.42	91.88

Calibration equation in form of y = bx + a; m Number of calibration points; R^2 Coefficient of determination, s_a Intercept standard deviation; s_b Slope standard deviation; $s_{y/x}$ Residuals standard deviation; LD_{sblank} Limit of detection calculated by the standard deviation of five determinations of a blank; For the NO estimated concentrations the error is the 95 % confidence interval calculated by the interpolated standard deviation; LQ Limit of quantification

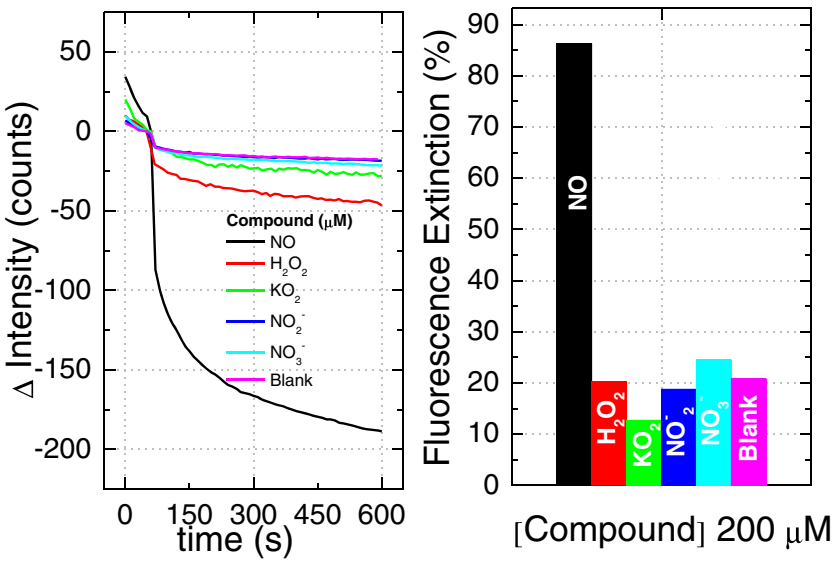

Fig. 10 Comparison of NO fluorescence time profile (**a**) and fluorescence extinction (**b**) with the principal ROS/RNS and NO similar compounds at concentration 200 μM

the selectivity of the CS-CdSe-MSA nanocomposite - 200 μM of each of the compounds were added. In Fig. 10 it is presented the reaction time profile and the percentage of fluorescence extinction for the assessed substances.

From the analysis of Fig. 10 it is possible to observe that only for NO a marked quenching effect on the fluorescence intensity of CS-CdSe-MSA is observed. The decrease of fluorescence intensity with the other evaluated compounds is in the same order to that found with the blank. The fluorescence decrease of the blank and mostly of the fluorescence decrease of the other compounds is probably due to the dilution effect by the increase of the volume added.

Conclusions

New CS-CdSe-MSA nanocomposites were synthesized and were evaluated for the NO detection and/or quantification. Synthetized CS-CdSe-MSA nanocomposite with a regular spherical shape and a size 4.19 nm were obtained. The detection of NO trough the quenching CS-CdSe-MSA fluorescence nanocomposite was verified. A wide linear concentration range 5 – 200 μM, good linear fit (R=0.997) and a lower limit of detection (1.86 μM) were found.

The CS-CdSe-MSA sensor adequately quantifies the NO in a DEA/NO solution. Slightly lowers recoveries were found with the NO standard solutions. Comparing the response of NO with the principal ROS/RNS and NO similar compounds no marked interferences are observed. Due to the proved NO detection and quantification capabilities and potentially good biocompatibility it is expected that the CS-CdSe-MSA nanocomposites could have biological applications.

Acknowledgments Financial support from Fundação para a Ciência e Tecnologia (FCT, Lisbon) project PEST and a PhD grant to Eliana Simões SFRH/BD/81074/2011 is acknowledged. The TEM analyses are also acknowledged to Jorge Nunes and group of de Nanomateriais e Microfabricação of CEMUC.

References

1. Valko M, Leibfritz D, Moncol J, Cronin MT, Mazur M, Telser J (2007) Free radicals and antioxidants in normal physiological functions and human disease. Int J Biochem Cell Biol 39: 44–84
2. Schoenfisch EM, Ha MH (2009) Analytical Chemistry of Nitric Oxide. Annu Rev Anal Chem (Palo Alto Calif) 2:409–433
3. Tarpey MM, Wink DA, Grisham MB (2004) Methods for detection of reactive metabolites of oxygen and nitrogen: in vitro and in vivo considerations. Am J Physiol Regul Integr Comp Physiol 286:R431–R444
4. Tarpey MM, Fridovich I (2001) Methods of detection of vascular reactive species: nitric oxide, superoxide, hydrogen peroxide, and peroxynitrite. Circ Res 89:224–236
5. Taha Z (2003) Nitric oxide measurements in biological samples. Talanta 61:3–10
6. Simões EFC, Leitão JMM, Barbosa RM, Esteves da Silva JCG (2012) Flow injection analysis for nitric oxide quantification based on reduced fluoresceinamine. Anal Methods 4:1089
7. Duarte AJ, Esteves da Silva JCG (2010) Reduced fluoresceinamine as a fluorescent sensor for nitric oxide. Sensors (Basel) 10:1661–1669
8. Ding L, Fan C, Zhong Y, Li T, Huang J (2013) A sensitive optic fiber sensor based on CdSe QDs fluorophore for nitric oxide detection. Sensors Actuators B Chem 185:70–76
9. Tan L, Wan A, Li H, Zhang H, Lu Q (2012) Biocompatible quantum dots–chitosan nanocomposites for fluorescence detection of nitric oxide. Mater Chem Phys 134:562–566
10. Fabregat V, Izquierdo MA, Burguete MI, Galindo F, Luis SV (2012) Quantum dot–polymethacrylate composites for the analysis of NOx by fluorescence spectroscopy. Inorg Chim Acta 381: 212–217

11. Yan XQ, Shang ZB, Zhang Z, Wang Y, Wei JJ (2009) Fluorescence sensing of nitric oxide in aqueous solution by triethanolamine-modified CdSe quantum dots. Luminescence 24:255–259
12. Ivanisevic A, Reynolds MF, Burstyn JN, Ellis AB (2000) Photoluminescent properties of cadmium selenide in contact with solutions and films of metalloporphyrins: Nitric oxide sensing and evidence for the aversion of an analyte to a buried semiconductor-film interface. J Am Chem Soc 122:3731–3738
13. Wang S, Han M-Y, Huang D (2009) Nitric oxide switches on the photoluminescence of molecularly engineered quantum dots. J Am Chem Soc 131:11692–11694
14. Tan L, Wan A, Li H, Lu Q (2012) Novel quantum dots-carboxymethyl chitosan nanocomposite nitric oxide donors capable of detecting release of nitric oxide in situ. Acta Biomater 8:3744–3753
15. Macquarrie DJ, Hardy JJE (2005) Applications of functionalized chitosan in catalysis. Ind Eng Chem Res 44:8499–8520
16. Mansur HS, Mansur AAP, Curti E, De Almeida MV (2013) Functionalized-chitosan/quantum dot nano-hybrids for nanomedicine applications: towards biolabeling and biosorbing phosphate metabolites. J Mater Chem B 1:1696–1711
17. Jiang R, Zhu H, Yao J, Fu Y, Guan Y (2012) Chitosan hydrogel films as a template for mild biosynthesis of CdS quantum dots with highly efficient photocatalytic activity. Appl Surf Sci 258:3513–3518
18. Zhan Li YD, Zhang Z, Pang D (2003) Preparation and characterization of CdS quantum dots chitosan biocomposite. React Funct Polym 55:35–43
19. Bezerra MA, Santelli RE, Oliveira EP, Villar LS, Escaleira LA (2008) Response surface methodology (RSM) as a tool for optimization in analytical chemistry. Talanta 76:965–977
20. Leitao JM, Esteves da Silva JC (2008) Factorial analysis optimization of a Diltiazem kinetic spectrophotometric quantification method. Anal Chim Acta 609:1–12
21. Lakowicz JR (2006) Principles of fluorescence spectroscopy. Springer, New York, pp 54–55